Journal of Organometallic Chemistry 694 (2009) 1400–1406

Contents lists available at ScienceDirect

Journal of Organometallic Chemistry

journal homepage: www.elsevier.com/locate/jorganchem

Syntheses, structural studies and spectroscopic characterisation of pyridyl–phthalimide complexes of *fac*-$(CO)_3Re^I$-diimines

Flora L. Thorp-Greenwood [a], Michael P. Coogan [a], Andrew J. Hallett [a], Rebecca H. Laye [b], Simon J.A. Pope [a,*]

[a] School of Chemistry, Main Building, Cardiff University, Park Place, Cardiff, Wales CF10 3AT, UK
[b] Department of Chemistry, University of Sheffield, Sheffield S3 7HF, UK

ARTICLE INFO

Article history:
Received 13 November 2008
Received in revised form 12 December 2008
Accepted 19 December 2008
Available online 16 January 2009

Keywords:
Rhenium
Diimine
Phthalimide
Luminescence

ABSTRACT

The mono-dentate ligands, 3-aminomethyl-*N*-phthalimido-pyridine (L^1) and 3-amino-*N*-phthalimido-pyridine (L^2), were synthesised using a solvent-free melt method. These ligands were then used to access three pairs of functionalised luminescent Re^I complexes of the generic type *fac*-{$Re(CO)_3$(diimine)(L^n)}(BF_4) [where diimine = 4,4′-dimethyl-2,2′-bipyridine (**dmb**); 2,2′-bipyridine (**bpy**); 1,10-phenanthroline (**phen**)]. X-ray crystallography has been used to structurally characterise five of the complexes showing that in the cases of the L^1 species the phthalimide unit is adjacent to and co-planar with the coordinated diimine ligand. Solution state UV–Vis absorption, electrochemistry and IR studies confirm that the proposed formulations and coordination modes exist in solution. The photophysical studies show that the visible emission from each of the six complexes is ^{3}MLCT at room temperature. Within each pair of complexes the precise energy of the emission was subtly dependent upon the axial ligand, L^n with luminescence lifetimes in the range 121–288 ns.

1. Introduction

Diimine complexes of the '*fac*-{$Re(CO)_3$}' core can be exploited as photoactive components within luminescent arrays allowing the design of multimetallic species [1] and responsive chemosensors [2]. More recently they have also been developed and utilised in biological fluorescence imaging applications where stepwise derivitisation allows tuning of the physical properties, exploitation of triplet metal(rhenium)-to-ligand(diimine) charge transfer (^{3}MLCT) emission [3] and elucidation of organelle targeting behaviour including mitochondrial localisation [4]. Such species are photophysically bio-compatible, allowing sensitisation in the visible region thus eradicating problematic endogenous autofluorescent backgrounds. Additional considerations are solubility and charge, to give lipophilic, cationic species allowing cell uptake, intracellular mobility and organelle localisation. In this study we report the syntheses of a series of cationic *fac*-{$Re(CO)_3$(diimine)-L^n}$^+$ complexes functionalised with a lipophilic, planar phthalimide unit tethered *via* a coordinated pyridine, which we hope will provide a useful basis for biologically applied studies in the future. Phthalimides are known to have potent biological activity [5] and the free ligands L^1 and L^2 utilised in this study have also demonstrated moderate promise in this regard [6] together with other *N*-pyridinyl and *N*-quinolinyl substituted phthalimides which have shown potent cytotoxicity towards several cultured cell lines [7]. Recent reports suggest utilising phthalimide derivatives to allow development of the '$Tc^I(CO)_3$' core with amino acid-based chelating ligands [8] for applications in positron emission tomography.

2. Synthesis

In contrast to the solvent-based reaction conditions previously employed for accessing these ligand systems, L^1 and L^2 were synthesised using a solvent-free melt method. Following recrystallisation from alcohol, yields were typically in excess of 90%. ^{1}H NMR spectra of the products were consistent with the proposed formulations and in agreement with the literature [6].

The neutral diimine precursors were synthesised according to the literature by reacting stoichiometric equivalents of pentacarbonlybromorhenium with either 2,2′-bipyridine, 4,4′-dimethyl-2,2′-bipyridine or 1,10-phenanthroline in toluene at 110 °C for 3 h [9]. Conversion to the cationic complexes was achieved by abstracting the axial bromide ligand with $AgBF_4$ in acetonitrile to yield the intermediate species *fac*-{$Re(CO)_3$(MeCN)(bisimine)}(BF_4) [10]. These were subsequently reacted with the pyridyl–phthalimide ligand (L^n) in chloroform at reflux. Typically the reaction was followed by thin layer chromatography (silica, 9:1 dichloromethane:methanol) and complete within 24 h. Column chromatography was not necessary to purify these complexes since the desired complex often precipitated directly from the cooled reaction mixture. Additional recrystallisation from acetonitrile/diethyl ether provided crystalline samples.

* Corresponding author. Tel.: +44 029 20879316; fax: +44 029 20874030.
E-mail address: popesj@cardiff.ac.uk (S.J.A. Pope).

0022-328X/$ - see front matter © 2009 Elsevier B.V. All rights reserved.
doi:10.1016/j.jorganchem.2008.12.048

3. Results and discussion

3.1. Characterisation of the complexes

Solution state IR studies (Fig. 3) were conducted in chloroform. For the *fac*-tricarbonyl core the local symmetry can be approximated to *Cs* and as a consequence three absorptions ($2A' + A''$) are expected although overlapping bands are common. Within each pair of diimine complexes the highest frequency ν(CO) band (CO *trans* to L^n) does not vary significantly with axial ligand type.

Electrospray mass spectrometry (positive mode) was utilised and for each complex revealed a cluster of peaks corresponding to the cationic unit, *i.e.* $\{Re(CO)_3(bisimine)(L^n)\}^+$, the isotopic distribution of which confirmed the presence of rhenium (^{185}Re, 37.1%; ^{187}Re 62.9%).

^{1}H NMR spectra were also obtained for each of the six complexes confirming the presence of the bisimine and pyridyl–phthalimide ligands within the Re^I coordination sphere.

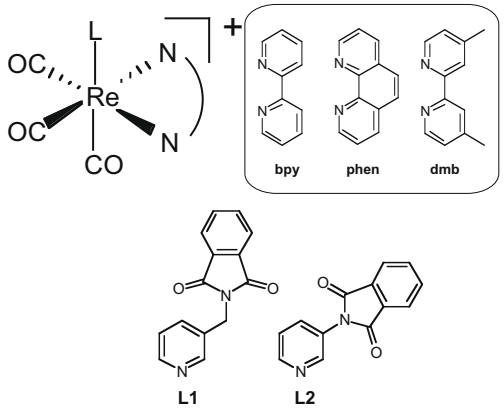

Scheme 1. Ligands and general cation of the rhenium complexes used in this study.

3.2. Single crystal X-ray diffraction studies of the complexes

Crystals representing each of the diimine types (*fac*-$\{Re(CO)_3(\mathbf{bpy})L^1\}(BF_4)$, *fac*-$\{Re(CO)_3(\mathbf{bpy})L^2\}(BF_4)$, *fac*-$\{Re(CO)_3(\mathbf{phen})L^1\}(BF_4)$, *fac*-$\{Re(CO)_3(\mathbf{phen})L^2\}(BF_4)$ and *fac*-$\{Re(CO)_3(\mathbf{dmb})L^2\}(BF_4)$) were isolated and deemed to be suitable for diffraction studies. In each case this was achieved by vapour diffusion of diethyl ether into a concentrated acetonitrile solution of the complex and crystals were grown over a period of 24 h. The parameters associated with each data collection are shown in Table 1, with associated bond lengths and bond angles in Supplementary material. In each case the structural analyses (Fig. 1) confirmed the proposed coordination geometry for rhenium with a *fac*-tricarbonyl arrangement supplemented with the chelating bisimine and axial *N*-coordinated pyridyl–phthalimide. The two examples incorporating the methyl-linked ligand L^1 show that the phthalimide unit is positioned adjacent to and co-planar with the diimine unit. In contrast, for the L^2 complexes the more rigid architecture positions the phthalimide unit away from the diimine. The bond lengths associated with the coordination sphere are typical of related Re^I complexes of this type [11]. Each of the Re–CO distances lies within the range 1.914–1.933 Å whilst the Re–N distances are typically longer at 2.159–2.225 Å. Generally, the Re–N bond lengths with the axial mono-dentate pyridine are longer (*ca.* 2.22 Å) than those associated with the chelating diimines (*ca.* 2.17 Å). The **bpy** complex with L^1 is more distorted (possibly due to the flexible tethered phthalimide unit and packing forces) from ideal octahedral symmetry ($\langle C_{ax}–Re–N_{ax}$ 175.95(13) vs. 178.89(13) for L^2 complex), which may account for a marginally weakened $Re–N_{ax}$ interaction. In comparison, analysis of the *fac*-$\{Re(CO)_3(\mathbf{phen})L^n\}(BF_4)$ structures shows that both are similarly distorted. *fac*-$\{Re(CO)_3(\mathbf{bpy})L^1\}(BF_4)$ and *fac*-$\{Re(CO)_3(\mathbf{phen})L^1\}(BF_4)$ show that when the diimine–Re bonding interaction is comparable, the axial Re–N is similarly bonded. Comparison of *fac*-$\{Re(CO)_3(\mathbf{bpy})L^2\}(BF_4)$ and *fac*-$\{Re\text{-}(CO)_3(\mathbf{dmb})L^2\}(BF_4)$ revealed that the stronger diimine–Re interaction of the latter results in a weakened $Re–N_{ax}$ bond. Therefore the factors determining the strength of the axial $Re–N_{ax}$(pyridyl) bond appear to be the donating ability of the diimine co-ligand and the inherent level of distortion within the coordination sphere.

Table 1
Crystal data collection and refinement details for the complexes[a].

	$\{Re(CO)_3(bpy)L^2\}(BF_4)$	$\{Re(CO)_3(bpy)L^1\}(BF_4)$	$\{Re(CO)_3(phen)L^1\}(BF_4)$	$\{Re(CO)_3(phen)L^2\}(BF_4)$	$\{Re(CO)_3(dmb)L^2\}(BF_4)$
Empirical formula	$C_{28}H_{19}BF_4N_5O_5Re$	$C_{29}H_{21}BF_4N_5O_5Re$	$C_{30}H_{20}BCl_2F_4N_4O_5Re$	$C_{30}H_{19}BF_4N_5O_5Re$	$C_{29}H_{24}BF_4N_4O_6Re$
Formula weight	778.49	792.52	860.41	802.51	797.53
T (K)	120(2)	120(2)	100(2)	100(2)	150(2)
Wavelength (Å)	0.71073	0.71073	0.71073	0.71073	0.71073
Crystal system	Monoclinic	Orthorhombic	Monoclinic	Monoclinic	Monoclinic
Space group	*P*2(1)/*c*	*Pbca*	P2(1)/*c*	*P*2(1)/*c*	*I*2/*a*
Unit cell dimensions					
a (Å)	12.1221(4)	16.0830(8)	13.184(3)	11.965(3)	21.428(2)
b (Å)	19.0972(5)	13.3736(7)	18.508(5)	18.992(4)	12.3526(13)
c (Å)	12.5934(4)	26.8120(14)	13.851(3)	13.153(3)	22.346(18)
α (°)	90.00	90.00	90.00	90.00°	90.00
β (°)	107.1890(10)	90.00	113.235(5)	106.249(11)	104.637(9)
γ (°)	90.00	90.00	90.00	90.00	90.00
V (Å^3)	2785.13(15)	5766.9(5)	3105.7(13)	2869.7(11)	5722.8(11)
Z	4	8	4	4	8
D_{calc}	1.857	1.826	1.840	1.858	1.851
Absorption coefficient	4.439	4.289	4.156	4.311	4.324
F(000)	1512	3088	1672	1560	3120
Crystal size (mm)	0.53 × 0.16 × 0.09	0.34 × 0.09 × 0.02	0.35 × 0.15 × 0.08	0.37 × 0.12 × 0.07	0.32 × 0.07 × 0.03
Reflections collected	6391	6641	7090	6639	6585
Independent reflections	5793	4690	6271	6028	5712
Goodness-of-fit on F	1.029	0.928	1.063	1.046	1.034
Final R indices [$I > 2\sigma(I)$]	R_1 = 0.0417, wR_2 = 0.1067	R_1 = 0.0257, wR_2 = 0.0534	R_1 = 0.0339, wR_2 = 0.0878	R_1 = 0.0192, wR_2 = 0.0451	R_1 = 0.0252, wR_2 = 0.0617
R indices (all data)	R_1 = 0.0444, wR_2 = 0.1083	R_1 = 0.0462, wR_2 = 0.0576	R_1 = 0.0392, wR_2 = 0.0909	R_1 = 0.0225, wR_2 = 0.0466	R_1 = 0.0324, wR_2 = 0.0656

[a] The structure was refined on F_o^2 using all data.

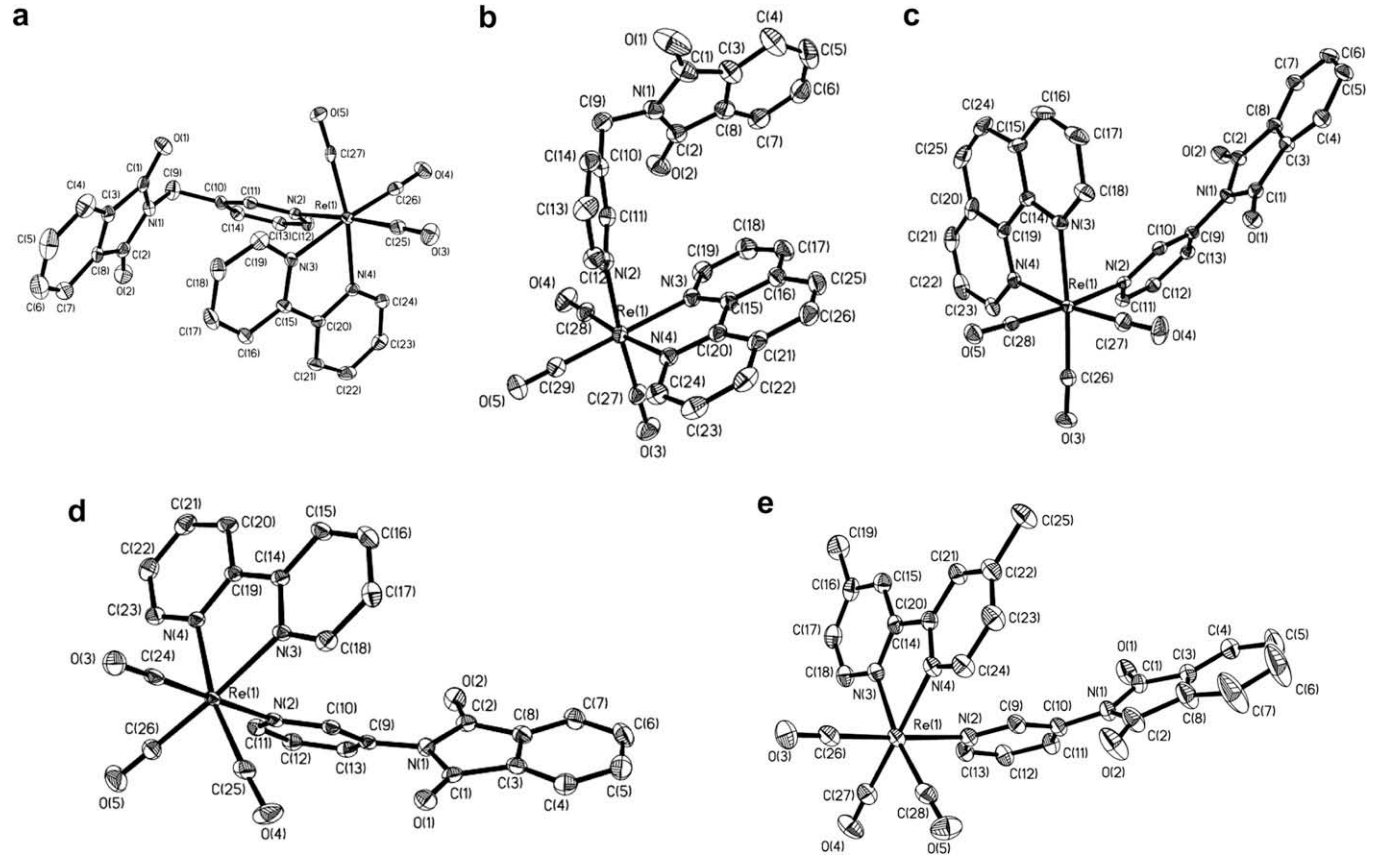

Fig. 1. Structural representations of the four complexes (a–e) *fac*-{Re(CO)$_3$(**bpy**)L^1}(BF$_4$), *fac*-{Re(CO)$_3$(**phen**)L^1}(BF$_4$), *fac*-{Re(CO)$_3$(**phen**)L^2}(BF$_4$), *fac*-{Re(CO)$_3$(**bpy**)L^2}(BF$_4$) and *fac*-{Re(CO)$_3$(**dmb**)L^2}(BF$_4$). Counter ions and solvent of crystallisation omitted for clarity, probability ellipsoids at 50%.

Table 2
IR, cyclic voltammetry, UV–Vis absorption, steady state and time-resolved luminescence: spectroscopic data associated with the complexes.

Complex	ν (CO)[a]	E_{ox}/V[b]	$-E_{red}/V$[b]	λ_{abs}/nm (ε/M^{-1} cm^{-1})[d]	^{3}MLCT emission maximum/nm[e]	^{3}MLCT τ/ns[f]
fac-{Re(CO)$_3$(bpy)L^1}(BF$_4$)	2037, 1929br	1.8	1.2°, 1.4	346 (4800), 319 (15300), 305 (16300), 266 (22800)	556	128
fac-{Re(CO)$_3$(bpy)L^2}(BF$_4$)	2036, 1937, 1929	–[g]	1.2[c], 1.4	340 (4600), 317 (14800), 305 (16000), 270 sh (22600)	548	148
fac-{Re(CO)$_3$(phen)L^1}(BF$_4$)	2034, 1936, 1924	1.8	1.2[c], 1.4, 2.0[c]	363 (4800), 324 sh (8300), 275 (34200)	543	281
fac-{Re(CO)$_3$(phen)L^2}(BF$_4$)	2034, 1935, 1924	1.8	1.2[c], 1.4	362 (4000), 321 sh (7800), 273 (32300)	539	266
fac-{Re(CO)$_3$(dmb)L^1}(BF$_4$)	2038, 1938br	1.8	1.3[c], 1.5, 2.1[c]	342 sh (5800), 315 (16700), 302 (18300), 266 (25800)	544	121
fac-{Re(CO)$_3$(dmb)L^2}(BF$_4$)	2037, 1939, 1928	1.8	1.2[c], 1.4, 2.1[c]	336 (4700), 315 (13100), 302 (14100), 270 sh (20900)	538	129

[a] In $CHCl_3$ solution.
[b] Referenced to Fc/Fc$^+$ in dry acetonitrile, scan rate of 200 mV/s.
[c] Irreversible.
[d] In acetonitrile solution.
[e] In aerated acetonitrile solution, λ_{ex} = 380 nm.
[f] In aerated acetonitrile solution, λ_{ex} = 372 nm.
[g] Difficult to obtain due to signal weakness and solvent window.

3.3. Electrochemistry

An investigation into the electrochemical behaviour of the six complexes was undertaken in de-aerated acetonitrile solution. The data associated with the oxidation potential of the rhenium centre (Re^{I}/Re^{II}) and the reduction potential of the diimine are presented in Table 2. With the anomolous exception of *fac*-{Re(CO)$_3$(**bpy**)L^2}(BF$_4$) for which we were unable to reliably record a value (due to the limitations of the solvent window at *ca.* +1.9 V) each of the complexes showed a reversible oxidation potential at around +1.8 V assigned to the Re$^{I/II}$ couple in line with previous observations [10]. Each of the complexes showed two or three reduction potentials which are usually assigned to diimine reduction and/or the Re$^{I/0}$ reduction. The first at *ca.* −1.2 V (−1.3 V for the less reducible **dmb** ligand) is assigned to the 0/−1 couple of the diimine ligands and was found to be irreversible for each complex. The second reduction at *ca.* −1.4 V was reversible in each case and attributed to the Re$^{I/0}$ couple. The complexes *fac*-{Re(CO)$_3$(**phen**)L^1}BF$_4$, *fac*-{Re(CO)$_3$(**dmb**)L^1}BF$_4$ and *fac*-{Re(CO)$_3$(**dmb**)L^2}BF$_4$ each showed a third irreversible reduction wave in the region −2.0 to −2.1 V. Although it is possible that this reduction may be due to a new species formed as a consequence of the first irreversible reduction process, the differing values may allow a tentative assignment to the 0/−1 couple of the pyridyl–phthalimide ligand

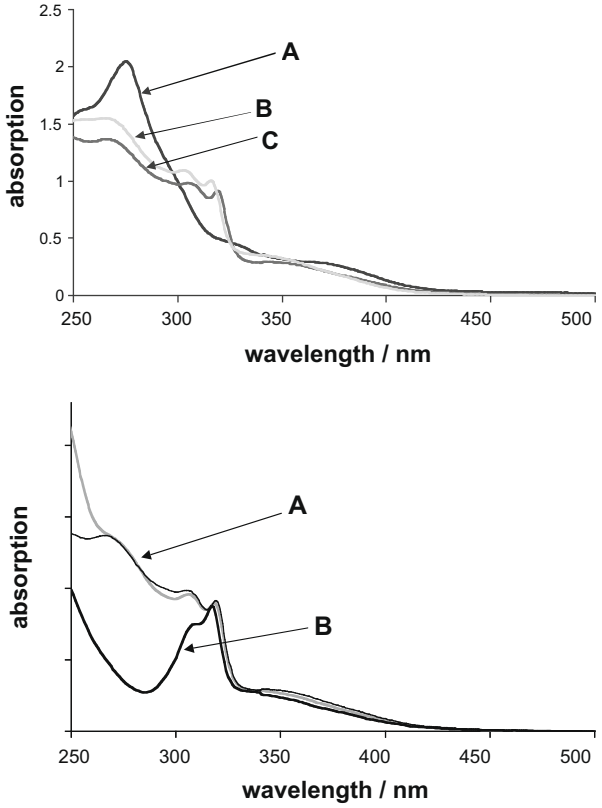

Fig. 2. Top: Electronic absorption spectra recorded with 2×10^{-4} M MeCN solutions. A, *fac*-{Re(CO)$_3$(**dmb**)L^2}(BF$_4$); B, *fac*-{Re(CO)$_3$(**phen**)L^2}(BF$_4$); C, *fac*-{Re(CO)$_3$(**bpy**)L^2}(BF$_4$). Bottom: normalised absorption spectra of A, superimposed *fac*-{Re(CO)$_3$(**bpy**)L^n}(BF$_4$); B, *fac*-{Re(CO)$_3$(**bpy**)MeCN}(BF$_4$).

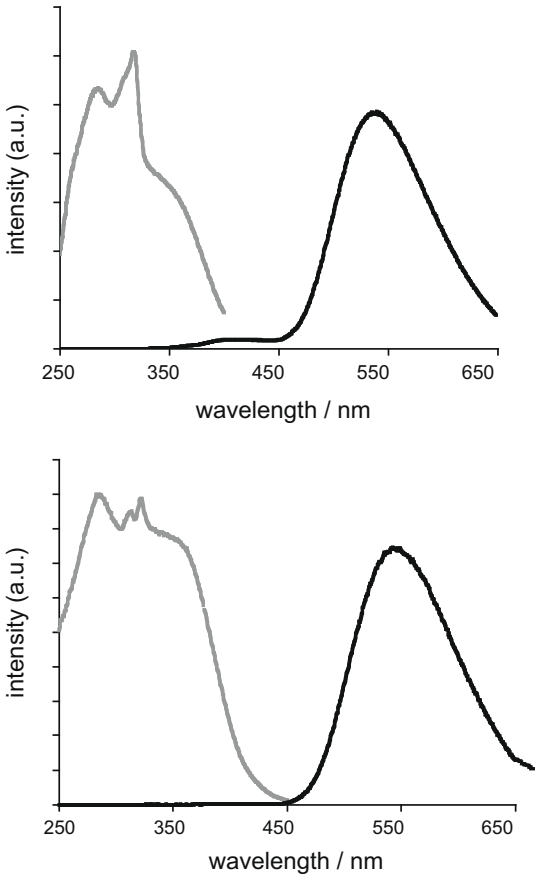

Fig. 3. Steady state excitation (grey) and emission (black, λ_{ex} = 285 nm) spectra for *fac*-{Re(CO)$_3$(**dmb**)L^n}(BF$_4$): L^2 (top), L^1 (bottom).

moiety, since phthalimides are known to undergo cathodic electrochemical reactions. Overall, the results show that electrochemically the rhenium centre is fairly insensitive to the changes in ligand type. The variation in reduction potentials of the bipyridine ligands within the pairs of **bpy** and **dmb** complexes, suggests that the variation in axial ligand L^n can subtly influence the electronic environment of the diimine, as suggested by the absorption and emission data.

3.4. Luminescence studies

Each of the target complexes possessed solution-state (MeCN) absorption characteristics consistent with the presence of both ligands in the rhenium coordination sphere (Fig. 2). Typically the lowest energy feature (>330 nm) appears as a broadened (often shoulder-like) transition and was assigned to a metal-to-ligand charge transfer (^{1}MLCT) d(Re) → π*(diimine) in accordance with previous studies [9a,10a]. The absorptions at shorter wavelengths 300–330 nm are attributed to the intraligand transitions of the bisimine moieties. As an example Fig. 2 shows a comparison of the absorption profiles of *fac*-{Re(CO)$_3$(**bpy**)L^n}(BF$_4$) with the precursor *fac*-{Re(CO)$_3$(**bpy**)MeCN}(BF$_4$). These spectra clearly demonstrate the additive effect of the axial pyridyl–phthalimide units to the absorption profile <300 nm which, as a consequence, are assigned to IL (singlet π → π* with the possibility of phthalimide $n \rightarrow \pi^*$) transitions.

The luminescence properties of the complexes were obtained on dilute (approximately 10^{-5} M) aerated acetonitrile solutions at room temperature. Firstly, steady state emission spectra were obtained by selective irradiation of the ^{1}MLCT transition using wavelengths >360 nm. In all six cases this resulted in a broad structureless emission band centred at *ca.* 550 nm consistent with ^{3}MLCT phosphorescence [9a,10a]. The precise λ_{em} positioning of the transition appeared to be ligand dependent: within each diimine class L^2 induced a subtle high energy shift for λ_{em} which was most pronounced for the **bpy** complexes. The degree of MLCT excited state stabilisation depends on the electron donating ability of the axial ligand [10a–e]: L^1 should be better able to donate electron density towards the virtual Re^{2+} centre of the excited state. The emission wavelength of both **phen** complexes was independent of excitation wavelength and thus assigned to conventional ^{3}MLCT [9a,10h,12]. Room temperature luminescence lifetime measurements of the complexes each gave single component decay consistent with a ^{3}MLCT assignment. τ_{MLCT} for the **bpy** and **dmb** derivatives was between 120 and 150 ns, whilst the phenathroline species were significantly longer-lived (despite possessing almost identical emission energies to the **dmb** species) reflecting the additional rigidity and limited excited state distortion inherent within the phenanthroline ligand, which consequently limit the vibrational deactivation pathways [10e]. However, although the **dmb** complexes possess higher emission energies than the **bpy** analogues, the resultant lifetimes are longer for the latter pair. Given that excited state distortion often increases with increasing excited state energy the vibrational deactivation of the **dmb** species may be more effective resulting in the shortened luminescence lifetimes [10e] (see Table 2).

The excitation spectra (probing the ^{3}MLCT emission band) obtained on 10^{-5} M solutions show significant variations with diimine type and axial ligand. Each of the spectra show bands assigned to MLCT transitions between 450 and 320 nm and defined

peaks at higher energies which can be attributed to intraligand transitions within the coordinated diimine ligand. There are differences in the spectra below 320 nm and thus it is also reasonable that, by comparison with the absorption spectra, some of these features can be assigned to the axial pyridyl–phthalimide ligands. These spectra demonstrate that subtle variations in the peripheral nature of the axial ligand can have an influence on the usable range of excitation wavelengths for the ^{3}MLCT emission (see Scheme 1).

Examples relating to chromophore-sensitised Re^I-based ^{3}MLCT emission are rare [13,14] although phthalimide chromophores have been utilised to sensitise the visibly luminescent lanthanide ions Tb(III) and Eu(III) [15]. Kahwa et al. showed that the excited triplet state energy of such chromophores was estimated as *ca.* 23 000 cm^{-1}. In our Re^I complexes photoinduced energy transfer is feasible on energetic grounds from either the phthalimide singlet or triplet states, given that the ^{3}MLCT lies at *ca.* 22 000 cm^{-1} (estimated from the ground and excited state 0–0 transition). Following excitation at 285 nm (in *fac*-{Re(CO)$_3$(**dmb**)L^n}(BF$_4$) pyridyl–phthalimide ligand contributes *ca.* 75% absorbance at 285 nm) ^{3}MLCT luminescence dominates, but for *fac*-{Re(CO)$_3$(**dmb**)L^2}(BF$_4$) there is a weak feature at *ca.* 418 nm attributed to residual pyridyl–phthalimide emission. Time-resolved analysis of this peak revealed τ_{flu} *ca.* 1.4 ns, consistent with a singlet fluorescence, which may be a consequence of trace contaminant of highly fluorescent free ligand, undetectable by other spectroscopic means. However, comparison to the photophysical properties of uncoordinated **L^2** (fluorescence lifetime in MeCN solution is *ca.* 2.0 ns at an emission maximum of 404 nm) more likely suggests that energy transfer from the singlet excited state of the chromophore may also contribute in these systems. Given that the energy transfer efficiency using either the Dexter or Förster mechanisms is strongly distance dependent (decreasing exponentially and by r^{-6}, respectively) it seems likely that the average intramolecular inter-chromophoric distance (*i.e.* phthalimide to diimine) is shorter in the complexes of L^1.

3.5. Conclusion

This paper reports the Re^I coordination chemistry of two pyridyl–phthalimide ligands to form cationic species of the general form *fac*-{Re(CO)$_3$(diimine)L^n}(BF$_4$). X-ray structural studies confirm both the coordination mode and geometry of the complexes. The strength of the pyridyl-rhenium interaction appears to be determined by the degree of distortion at the octahedral ion, which is more pronounced for the L^1 species. In each case the complexes possess visible ^{3}MLCT emission with luminescent lifetimes in excess of 120 ns. The electronic nature of the axial ligand produces subtle changes in the precise energy of the ^{3}MLCT emission, depending on the degree of excited state MLCT stabilisation. The quenching of phthalimide fluorescence suggests that photoinduced energy transfer can operate in these species, but that the potentially greater inter-chromophoric distance of the L^1 complexes may account for any observed residual fluorescence. Importantly this investigation shows that these rhenium complexes incorporating phthalimide-functionalised ligands retain their useful emission properties, exploiting a range of excitation wavelengths, and thus renders them attractive candidates in our ongoing investigation into the biological application of such complexes in confocal fluorescence microscopy.

3.6. Experimental

Materials: The neutral rhenium complexes, including ReBr(CO)$_5$ [16], and the cationic acetonitrile intermediates were prepared according to or based upon literature reports [10].

3.6.1. Synthesis of L^1

3-Picolylamine (1 g, 9.25 mmol) and phthalic anhydride (1.37 g, 9.25 mmol) were mixed in a test tube. The mixture was heated to a melt with a hot air gun with occasional agitation *via* glass rod. Moderate heating was continued until water vapour was produced and condensing on the test tube wall [care must be taken not to overheat the mixture and decompose the reactants and product]. Once water vapour was no longer evident, heating was stopped and the reaction mixture cooled. The mixture was added to hot ethanol (*ca.* 50 cm^3), filtered, and the resultant solute allowed to cool to room temperature. Upon cooling the product precipitated as a white crystalline solid. Further crops of product were isolated following concentration of the alcoholic solution and storage at 0 °C.

3.6.2. Synthesis of L^2

As for L^1, but using 3-aminopyridine (1 g, 10.6 mmol) and phthalic anhydride (1.57 g, 10.6 mmol).

3.6.3. Synthesis of fac-{Re(CO)$_3$(bpy)L^1}(BF$_4$)

The title compound was prepared by heating {Re(CO)$_3$(bpy)(NCCH$_3$)}(BF$_4$) (50 mg, 9.02×10^{-5} mol) and excess L^1 (25 mg, 1.05×10^{-4} mol) in chloroform (10 cm^3) under reflux in a nitrogen atmosphere for 48 h. The product was precipitated from an acetonitrile/diethyl ether mixture to give a pale yellow solid (29 mg, 43%). IR ν_{max} (CHCl$_3$, cm^{-1}) 1929, 1937, 2036. UV–Vis (MeCN) λ_{max} (ε/M^{-1} cm^{-1}) 346 (4800), 319 (15 300), 305 (16 300), 266 (22 800) nm. ^{1}H NMR (400 MHz, CDCl$_3$) δ_H 4.61 (2H, s, –C*H*$_2$), 7.28 (1H, m, py), 7.70 (4H, overlapping m, phth and bpy), 7.76 (2H, m, phth), 7.84 (1H, d, $^3J_{HH}$ = 8.1 Hz, py), 8.08 (1H, d, $^3J_{HH}$ = 5.1 Hz py), 8.23 (1H, s, py), 8.25 (2H, d, $^3J_{HH}$ = 8.1 Hz, bpy), 8.64 (2H, d, $^3J_{HH}$ = 8.1 Hz, bipy), 9.03 (2H, d, $^3J_{HH}$ = 4.5 Hz, bpy) ES$^+$ MS found *m/z* 665; calculated *m/z* 665 for {M+H−BF$_4$}$^+$. HR ESI found *m/z* 663.0805; C$_{27}$H$_{18}$O$_5$N$_4$^{185}Re requires 663.0801.

3.6.4. Synthesis of fac-{Re(CO)$_3$(bpy)L^2}(BF$_4$)

As above, but using {Re(CO)$_3$(bpy)(NCCH$_3$)}(BF$_4$) (50 mg, 9.02×10^{-5} mol) and excess L^2 (25 mg, 1.12×10^{-4} mol) and chloroform (10 cm^3). A sandy brown coloured solid was isolated (28 mg, 44%). IR ν_{max} (CHCl$_3$, cm^{-1}) 1929, 2037. UV–Vis (MeCN) λ_{max} (ε/M^{-1} cm^{-1}) 340 (4600), 317 (14 800), 305 (16 000), 270 sh (22 600) nm. ^{1}H NMR (400 MHz, MeOD) δ_H 7.45 (1H, m, py), 7.79–7.85 (6H, overlapping m, phth and bpy), 8.08 (1H, d, $^3J_{HH}$ = 7.8 Hz, py), 8.22 (1H, m, py), 8.25 (2H, m, bpy), 8.48 (1H, s, py), 8.52 (2H, d, $^3J_{HH}$ = 8.0 Hz, bpy), 9.22 (2H, d, $^3J_{HH}$ = 7.6 Hz, bpy). ES$^+$ MS found *m/z* 651; calculated *m/z* 651 for {M+H−BF$_4$}$^+$. HR ESI found *m/z* 649.0641; C$_{26}$H$_{16}$O$_5$N$_4$^{185}Re requires 649.0645.

3.6.5. Synthesis of fac-{Re(CO)$_3$(phen)L^1}(BF$_4$)

The title compound was prepared by heating equimolar quantities of {Re(CO)$_3$(phen)(NCCH$_3$)}(BF$_4$) (30 mg, 5.19×10^{-4} mol) and L^1 (12 mg, 5.19×10^{-4} mol) in chloroform (10 cm^3) under N$_2$ for 48 h. The product was precipitated from acetonitrile using diethyl ether to give a pale yellow solid (75 mg, 77%). IR ν_{max} (CHCl$_3$, cm^{-1}) 1928, 1939, 2037. UV–Vis (MeCN) λ_{max} (ε/M^{-1} cm^{-1}) 363 (4800), 324 sh (8300), 275 (34 200) nm. ^{1}H NMR (250 MHz, MeOD) δ_H 4.48 (2H, s, –C*H*$_2$), 7.59 (1H, m, py), 7.65 (2H, m, phth), 7.74 (2H, m, phth), 7.81 (2H, s, phen), 8.03 (1H m, py), 8.08 (2H, m, phen), 8.29 (1H, d, py, $^3J_{HH}$ = 5.02 Hz), 8.44 (1H, d, py, $^3J_{HH}$ = 4.7 Hz), 8.77 (2H, dd, J_{HH} = 8.3, 1.3 Hz, phen), 9.59 (2H, dd, J_{HH} = 5.2, 1.4 Hz, phen). ES$^+$ MS found *m/z* 689, calculated *m/z* 689 for {M+H−BF$_4$}$^+$. HR ESI found *m/z* 687.0808; C$_{29}$H$_{18}$O$_5$N$_4$^{185}Re requires 687.0801.

3.6.6. Synthesis of fac-{Re(CO)$_3$(phen)L^2}(BF$_4$)

The title compound was prepared by heating equimolar quantities of {Re(CO)$_3$(phen)(NCCH$_3$)}(BF$_4$) (20 mg, 3.46×10^{-5} mol) and

L^2 (8 mg, 3.46×10^{-5} mol) in chloroform (10 cm^3) under reflux in a nitrogen atmosphere overnight to give a yellow solid (14 mg, 53%) which precipitated from the reaction medium. IR ν_{max} ($CHCl_3$, cm^{-1}) 1938, 2038. UV–Vis (MeCN) λ_{max} ($\varepsilon/M^{-1}\,cm^{-1}$) 362 (4000), 321 sh (7800), 273 (32300) nm. ^1H NMR (400 MHz, MeOD) δ_H 7.18 (1H, m, Py), 7.3–7.8 (5H, overlapping multiplet, phth (4H) and py (1H)), 8.10 (2H, m, phen), 8.15 (2H, s, phen), 8.26 (1H, d, $^3J_{HH}$ = 5.2 Hz, py), 8.85 (2H, dd, J = 8.3, 1.1 Hz, phen), 8.89 (1H, s, py), 9.62 (2H, dd, J = 5.1, 1.1 Hz, phen). ES^+ MS found m/z 675, calculated m/z 675 for $\{M+H-BF_4\}^+$. HR ESI found m/z 673.0640; $C_{28}H_{16}O_5N_4{}^{185}Re$ requires 673.0645.

3.6.7. Synthesis of fac-{Re(CO)$_3$(dmb)L^1}(BF$_4$)

The title compound was prepared by heating equimolar quantities of $\{Re(CO)_3(dmb)(NCCH_3)\}(BF_4)$ (20 mg, 3.46×10^{-5} mol) with L^1 (8 mg, 3.46×10^{-5} mol) in chloroform (10 cm^3) under reflux in a nitrogen atmosphere, overnight. The yellow solution was dried and dissolved in methanol (1 cm^3) the product precipitated using diethyl ether (5 cm^3) to give a pale yellow solid (28 mg, 53%). IR ν_{max} ($CHCl_3$, cm^{-1}) 1924, 1935, 2034. UV–Vis (MeCN) λ_{max} ($\varepsilon/M^{-1}\,cm^{-1}$) 342 (5800), 315 (13100), 302 (18300), 266 (25800) nm. ^1H NMR (400 MHz, $CDCl_3$) δ_H 2.56 (6H, s, 2 × –CH_3), 4.62 (2H, s, –CH_2), 7.27 (1H, m, py), 7.44 (2H, d, $^3J_{HH}$ = 5.5 Hz, bpy), 7.69 (2H, m, phth), 7.76 (2H, m, phth), 7.84 (1H, d, $^3J_{HH}$ = 8.0 Hz, py), 8.00 (1H, d, $^3J_{HH}$ = 4.9 Hz, py), 8.27 (1H, s, py), 8.49 (2H, s, bipy), 8.82 (2H, d, $^3J_{HH}$ = 5.7 Hz, bpy). ES^+ MS found m/z 693, calculated m/z 693 for $\{M+H-BF_4\}^+$. HR ESI found m/z 691.1113; $C_{29}H_{22}O_5N_4{}^{185}Re$ requires 691.1114.

3.6.8. Synthesis of fac-{Re(CO)$_3$(dmb)L^2}(BF$_4$)

The title compound was prepared by heating was prepared by heating equimolar quantities of $\{Re(CO)_3(dmb)(NCCH_3)\}(BF_4)$ (20 mg, 3.43×10^{-5} mol) and L^2 (8 mg, 3.43×10^{-5} mol) in chloroform (10 cm^3) under reflux in a nitrogen environment overnight. The yellow solid was precipitated with diethyl ether. IR ν_{max} ($CHCl_3$, cm^{-1}) 1924, 1936, 2034. UV–Vis (MeCN) λ_{max} ($\varepsilon/M^{-1}\,cm^{-1}$) 336 (4700), 315 (13100), 302 (14100), 270 sh (20900) nm. ^1H NMR (400 MHz, MeOD) δ_H 2.51 (6H, s, 2 × –CH_3), 7.24 (1H, m, py), 7.3–7.7 (6H, overlapping multiplet, bpy (2H), phth (4H)), 7.88 (1H, d, $^3J_{HH}$ = 5.5 Hz, py), 8.19 (1H, d, $^3J_{HH}$ = 4.9 Hz, py), 8.40 (2H, s, bpy), 8.89 (1H, s, py), 9.02 (2H, d, $^3J_{HH}$ = 6.1 Hz, bpy). ES^+ MS found m/z 679, calculated m/z 679 for $\{M+H-BF_4\}^+$. HR ESI found m/z 677.0955; $C_{28}H_{20}O_5N_4{}^{185}Re$ requires 677.0958.

4. General physical measurements

All photophysical data were obtained on a JobinYvon-Horiba Fluorolog spectrometer fitted with a JY TBX picosecond photodetection module. Emission spectra were uncorrected and excitation spectra were instrument corrected. The pulsed source was a NanoLED configured for 372 nm output operating at 500 kHz. Luminescence lifetimes were obtained using the JY-Horiba FluorHub single photon counting module. IR spectra were recorded on a Varian 7000 FT-IR spectrometer. Low resolution mass spectra were obtained using a Bruker MicroTOF LC. UV–Vis spectra were recorded using a Jasco 630 UV–Vis spectrophotometer. Electrochemical studies were carried out using a Parstat 2273 potentiostat in conjunction with a three-electrode cell. The auxiliary electrode was a platinum wire and the working electrode a platinum (1.0 mm diameter) disc. The reference was a silver wire separated from the test solution by a fine-porosity frit. Solutions (10 ml CH_3CN) were 0.1×10^{-3} mol dm^{-3} in the test compound and 0.1 mol dm^{-3} in $[NBu_4][PF_6]$ as the supporting electrolyte. Solutions were deoxygenated with a stream of N_2 gas and were maintained under a positive pressure of N_2 during all measurements. Potentials are quoted vs. the $[Fe(\eta^5\text{-}C_5H_5)_2]^+/[Fe(\eta^5\text{-}C_5H_5)_2]$ couple (E° = +0.39 V in CH_3CN) as the internal standard.

5. Data collection and processing

Crystal data, data collection and refinement parameters for the complexes are given in Table 1; selected bond lengths and angles in Supplementary material. Diffraction data were collected on a Bruker KAPPA APEX 2 using graphite-monochromated Mo Kα radiation (k = 0.71073 Å) at 100, 120 or 150 K. Software package APEX 2 (v2.1) was used for the data integration, scaling and absorption correction.

6. Structure analysis and refinement

The structure was solved by direct methods using SHELXS-97 and was completed by iterative cycles of ΔF-syntheses and full-matrix least squares refinement. All non-H atoms were refined anisotropically and difference Fourier syntheses were employed in positioning idealised hydrogen atoms and were allowed to ride on their parent C-atoms. All refinements were against F^2 and used SHELX-97.[17]

Acknowledgements

We thank the Universities of Cardiff and Sheffield for support. EPSRC are also thanked for financial support. Prof. Michael D. Ward (University of Sheffield) is acknowledged for granting access to X-ray crystallographic facilities. We also recognise the efforts of the EPSRC Mass Spectrometry National Service at the University of Swansea.

Appendix A. Supplementary material

CCDC 703241, 703242, 703243, 703244 and 703245 contain the supplementary crystallographic data for *fac*-{Re(CO)$_3$(**phen**)(L^1)}(BF$_4$), *fac*-{Re(CO)$_3$(**bpy**)(L^2)}(BF$_4$), *fac*-{Re(CO)$_3$(**dmb**)(L^2)}(BF$_4$), *fac*-{Re(CO)$_3$(**bpy**)(L^1)}(BF$_4$) and *fac*-{Re(CO)$_3$(**phen**)(L^2)}(BF$_4$). These data can be obtained free of charge from The Cambridge Crystallographic Data Centre via www.ccdc.cam.ac.uk/data_request/cif. Supplementary data associated with this article can be found, in the online version, at doi:10.1016/j.jorganchem.2008.12.048.

References

[1] (a) For examples: C.R.K. Glasson, L.F. Lindoy, G.V. Meehan, Coord. Chem. Rev. 252 (2008) 940;
(b) K.S. Schanze, D.B. MacQueen, T.A. Perkins, L.A. Cabana, Coord. Chem. Rev. 122 (1993) 63;
(c) N.B. Thornton, K.S. Schanze, Inorg. Chem. 32 (1993) 4994;
(d) T.L. Easun, W.Z. Alsindi, M. Towrie, K.L. Ronayne, X.Z. Sun, M.D. Ward, M.W. George, Inorg. Chem. 47 (2008) 5071;
(e) N.M. Shavaleev, Z.R. Bell, M.D. Ward, Dalton Trans. (2002) 3925;
(f) S.J.A. Pope, B.J. Coe, S. Faulkner, Chem. Commun. (2004) 1501;
(g) Y. Fan, L.Y. Zhang, F.R. Dai, L.X. Shi, Z.N. Chen, Inorg. Chem. 47 (2008) 2811;
(h) R. Argazzi, E. Bertolasi, C. Chioboli, C.A. Bignozzi, M.K. Itokazu, N.Y. Murakami Iha, Inorg. Chem. 40 (2001) 6885.
[2] (a) For examples: D. Pelleteret, N.C. Fletcher, A.P. Doherty, Inorg. Chem. 46 (2007) 4386;
(b) K.K.W. Lo, W.K. Hui, Inorg. Chem. 44 (2005) 1992;
(c) J.D. Lewis, J.N. Moore, Chem. Commun. (2003) 2858;
(d) D.R. Cary, N.P. Zaitseva, K. Gray, K.E. O'Day, C.B. Darrow, S.M. Lane, T.A. Peyser, J.H. Satcher Jr., W.P. Van Antwerp, A.J. Nelson, J.G. Reynolds, Inorg. Chem. 42 (2002) 1662;
(e) H.D. Stoeffler, N.B. Thornton, S.L. Temkin, K.S. Schanze, J. Am. Chem. Soc. 117 (1995) 7119;
(f) X.Q. Guo, F.N. Castellano, L. Li, H. Szmacinski, J.R. Lakowicz, J. Sipior, Anal. Biochem. 254 (1997) 179;
(g) V.W.W. Yam, A.S.F. Kai, Chem. Commun. (1998) 109;

(h) J.N. Demas, B.A. DeGraff, Coord. Chem. Rev. 211 (2001) 317;
(i) M.H. Keefe, K.D. Benkstein, J.T. Hupp, Coord. Chem. Rev. 205 (2000) 201;
(j) P.D. Beer, S.W. Dent, Chem. Commun. (1998) 825;
(k) P. de Wolf, S.L. Heath, J.A. Thomas, Chem. Commun. (2002) 2540.
[3] A.J. Amoroso, M.P. Coogan, J.E. Dunne, V. Fernández-Moreira, J. Hess, A.J. Hayes, D. Lloyd, C. Millet, S.J.A. Pope, C. Williams, Chem. Commun. (2007) 3066.
[4] A.J. Amoroso, M.P. Coogan, V. Fernández-Moreira, A.J. Hayes, D. Lloyd, C. Millet, S.J.A. Pope, New J. Chem. 32 (2008) 1097.
[5] S.M. McHugh, T.L. Rowland, Clin. Exp. Immun. 110 (1997) 151.
[6] X. Collin, J.-M. Robert, G. Wielgosz, G. Le Baut, C. Bobin-Dubigeon, N. Grimaud, J.-Y. Petit, Eur. J. Med. Chem. 36 (2001) 639.
[7] E.A. Carswell, I.J. Old, R.L. Kassel, S. Green, N. Foire, B. Williamson, Proc. Natl. Acad. Sci. USA 72 (1975) 3666.
[8] (a) S.R. Banerjee, J.W. Babich, J. Zubieta, Inorg. Chem. Commun. 7 (2004) 481;
(b) S.R. Banerjee, K.P. Maresca, L. Francesconi, J. Valliant, J.W. Babich, J. Zubieta, Nucl. Med. Biol. 32 (2005) 1.
[9] (a) M. Wrighton, D.L. Morse, J. Am. Chem. Soc. 96 (1974) 998;
(b) A. Juris, S. Campagna, I. Bidd, J.-M. Lehn, R. Ziessel, Inorg. Chem. 27 (1988) 4007;
(c) D.R. Cary, N.P. Zaitseva, K. Gray, K.E. O'Day, C.B. Darrow, S.M. Lane, T.A. Peyser, J.H. Satcher Jr., W.P. Van Antwerp, A.J. Nelso, J.G. Reynolds, Inorg. Chem. 41 (2002) 1662.
[10] (a) L. Sacksteder, A.P. Zipp, E.A. Brown, J. Streich, J.N. Demas, B.A. DeGraff, Inorg. Chem. 29 (1990) 4335;
(b) J.V. Caspar, B.P. Sullivan, T.J. Meyer, Inorg. Chem. 23 (1984) 2104;
(c) A.P. Zipp, L. Sacksteder, J. Streich, A. Cook, J.N. Demas, B.A. DeGraff, Inorg. Chem. 32 (1993) 5629;
(d) L. Sacksteder, M. Lee, J.N. Demas, B.A. DeGraff, J. Am .Chem. Soc. 115 (1993) 8230;
(e) D.J. Stufkens, A. Vlcek Jr., Coord. Chem. Rev. 177 (1998) 127;
(f) A.J. Lees, Chem. Rev. 87 (1987) 711;
(g) C.-C. Ko, L.-X. Wu, K. Man-Chung Wong, N. Zhu, V.W.-W. Yam, Chem. Eur. J. 10 (2004) 766;
(h) S.M. Fredericks, J.C. Luong, M.S. Wrighton, J. Am. Chem. Soc. 101 (1979) 7415.
[11] (a) N.M. Shavaleev, A. Barbieri, Z.R. Bell, M.D. Ward, F. Barigelletti, New J. Chem. 28 (2004) 398;
(b) S. Belanger, M. Gilbertson, D.I. Yoon, C.L. Stern, X. Dang, J.T. Hupp, Dalton Trans. (1999) 3407;
(c) L.A. Mullice, R.H. Laye, L.P. Harding, N.J. Buurma, S.J.A. Pope, New J. Chem. 32 (2008) 2140.
[12] (a) D.R. Striplin, G.A. Crosby, Coord. Chem. Rev. 211 (2001) 163;
(b) D.R. Striplin, G.A. Crosby, Chem. Phys. Lett. 221 (1994) 426.
[13] N.M. Shavaleev, Z.R. Bell, T.L. Easun, R. Rutkaite, L. Swanson, M.D. Ward, Dalton Trans. (2004) 3678.
[14] Dirksen U. Hahn, F. Schwanke, M. Nieger, J.N.H. Reek, F. Vogtle, L. De Cola, Chem. Eur. J. 10 (2004) 2036.
[15] D.M.Y. Barrett, I.A. Kahwa, B. Raduchel, A.J.P. White, D.J. Williams, Perkin Trans. 2 (1998) 1851.
[16] S.P. Schmidt, W.C. Trocler, F. Basolo, Inorg. Synth. 28 (1990) 160.
[17] SHELXL-PC Package. Bruker Analytical X-ray Systems: Madison, WI, 1998.